Structural investigations of multiple gratings recorded in polymer-dispersed liquid crystals film by holography

Zhigang Zheng[a]; Lishuang Yao[b]; Li Xuan[b]; Dong Shen[a]

[a] Department of Physics, East China University of Science and Technology, Shanghai, China [b] State Key Laboratory of Applied Optics, Changchun Institute of Optics, Fine Mechanics and Physics, Chinese Academy of Science, Changchun, China

PLEASE SCROLL DOWN FOR ARTICLE

Structural investigations of multiple gratings recorded in polymer-dispersed liquid crystals film by holography

Zhigang Zheng[a], Lishuang Yao[b], Li Xuan[b] and Dong Shen[a]*

[a]*Department of Physics, East China University of Science and Technology, Shanghai, China;* [b]*State Key Laboratory of Applied Optics, Changchun Institute of Optics, Fine Mechanics and Physics, Chinese Academy of Science, Changchun, China*

Angular multiple transmission gratings were recorded simultaneously in acrylate-based polymer-dispersed liquid crystals film by holography. The micro-structure of the gratings was investigated through atomic force microscopy and scanning electron microscopy, and we found that with the exception of the holographic volume structure, each grating has a surface relief with the depth of tens of nanometres. The effects of surface relief on the optical and electrical performances of the multiple gratings were tested, and the results indicate that the diffraction efficiency of multiple gratings is mainly determined by the refractive index modulation of the volume structure; however, the diffraction energy of surface relief is less than 5% of the total. The results show no evident influence of the surface relief on Bragg angle and drive electric field. Through experimental analysis, it is also shown that volume shrinkage of about 2% for the gratings occurs after exposure. In addition, multiple images were recorded in this work, the readout and erasing performances were tested, and the transmission of the sample in visible spectrum was detected; our results indicate a prospective application for holographic polymer-dispersed liquid crystal film in displays or data storage.

Keywords: polymer-dispersed liquid crystals; structure; image storage

1. Introduction

With the development of the information industry and communication technology, data storage and transfer issues become more and more important. The mainstream method which is normally adopted to enable data storage is multiple holographic recording, not only because the technology of holography is mature, but also for the light and space saving of holograms. From the 1990s, much research focussed on multiple recording was carried out [1–6]. New applications for multiple holography in substrate waveguide [3] and optical interconnection [4] were proposed. The recording emulsions used in these works are mainly dichromated gelatin or other crystals [5, 6]. Gambogi *et al*. utilised DuPont photopolymers as the holographic recording medium; the claimed advantages of photopolymers over other conventional types of emulsion include dry-processing capability, long shelf life and good photo-speed [7]. In addition, much effort has been focussed in recent years on the dynamics of photopolymers in the processing of holographic formations [1, 2, 8].

Polymer-dispersed liquid crystals (PDLC) is a kind of new functional material which can be fabricated by photopolymerising a mixture of photosensitive monomers and nematic liquid crystals, forming a polymer-enclosed liquid crystal film [9]. Due to the electromagnetic response of LCs, the optical properties of such films can be tuned by electric or magnetic fields. If the material is used as a holographic medium, some specific optical devices, such as the grating or image storage, can be achieved, based on the fundamental principle of photo-initiated polymerisation-induced phase separation (PIPS), which promotes the formation of polymer-rich and LC-rich zones [10]. This is the so-called holographic polymer-dispersed liquid crystal (HPDLC), initially proposed by Sutherland *et al*. in 1993 [11]. Compared with the conventional emulsions, HPDLC is more favourable for multiple recording, as its unusual tunability is necessary in light amplifiers and displays. Although some kinds of holographic devices based on azobenzene materials can also be switched by virtue of reversible trans-cis-trans isomerisation [12–14], there are some insurmountable barriers compared with HPDLC, such as the very slow response and structural instability.

The first multiple HPDLC was reported by Bowley *et al*. in the year 2000. They recorded three gratings simultaneously in the film; however, due to various physical and chemical problems, or interactions between them, the morphology and optical properties of the hologram were not satisfied. The diffraction efficiency was less than 20% and the interface

---

*Corresponding author. Email: shen@ecust.edu.cn

between polymer-rich and LC-rich zones was hard to discern [15]. To understand the mechanisms of these problems and improve the basic performance of holograms, researchers have focussed their efforts on the dynamics occurring during the formation of HPDLCs. Some studies, looking at the LC/polymer ratio, recording intensity, and recording methodology, have been reported in recent years [16–18]. However, the micro-structure of multiple HPDLCs, which directly determines the optical performance of the hologram, has rarely been studied. Although some researchers have reported their morphological observations through scanning electron microscopy (SEM) or optical microscopy, there has been no discussion of the detailed effects on optical or electrical behaviours [19, 20].

In this paper, two angular multiple transmission gratings were recorded simultaneously in a single HPDLC film. The structures of the gratings were observed with atomic force microscopy (AFM) and SEM, and analysed through Bragg's law. The diffraction efficiency and electro-optical performance were tested, and the effects of structures on them are discussed. Finally, two black and white images were recorded in HPDLC film. The images can be erased by applying a certain voltage, and some other optical properties are also investigated experimentally.

2. Experimental details

2.1 Preparation of materials

Two main materials were used to prepare HPDLC: commercial nematic liquid crystals (TEB30A, $n_o =$ 1.5222 $\Delta n = 0.1703$, $T_{NI} = 61.2°C$, Slichem Co., Ltd. Shijiachuang, China) and conventional acrylate

monomers; their weight ratio was controlled at 3:7. The component of the monomers are penta-functional dipentaerythritol hydroxyl penta-acrylate (DPHPA, Aldrich) and di-functional phthalic diglycol diacrylate (PDDA, Eastern Acrylic Chem. Tech. Co., Ltd. Beijing), mixed uniformly with the weight ratio of 1:1. Small amounts of photoinitiator Rose Bengal and co-initiator n-phenylglycine were mixed together for the polymerisation at laser irradiation of 532 nm. To improve the morphological structure and decrease the drive voltage of the multiple HPDLC sample, about 4 wt% of fluorinated acrylate monomer, dodecafluoroheptyl methacrylate (XEOGIA Fluorine-Silicon Chem. Co., Ltd. Harbin) was added as the surfactant. The mixture is stirred at a temperature of over 40°C for more than 12 h, and then injected into the vacant cell with 12 μm-thick walls.

2.2 Holography setup

The cell was placed at the position labelled 'sample' in Figure 1. A beam with the wavelength of 532 nm was emitted from a YAG frequency doubling laser, expanded and filtered by the beam expander and pin hole, and then divided into four beams with the same intensity by three beam-splitters (labelled 'BS' in Figure 1). Two beams, L1 and L2, were reflected by the mirrors M2 and M3 with the cross-angle of 4.7° on the sample; the other two, K1 and K2, irradiated the sample with a larger cross-angle of 20°. The polarised planes of beams K1 and K2 were rotated 90° by the half-wave plate to avoid the coherence between beams Ki and Li (i = 1, 2). A He–Ne laser was used to detect the optical property of the multiple gratings. The beams incident from the other side of the sample
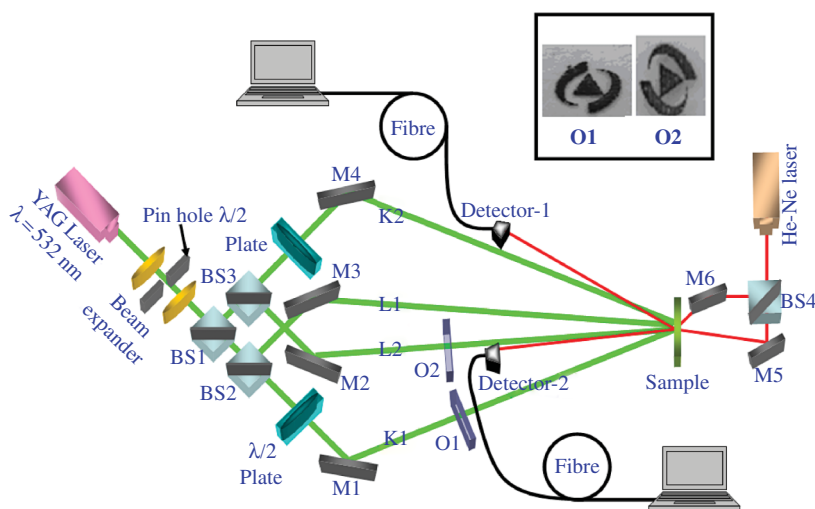

Figure 1. Holography setup in the experiments (colour version online).

with Bragg angle and the output signals were received by two detectors. All angles mentioned above have been converted to those inside the medium through Snell's law. At the end, two black and white transparent slices were placed at the positions labelled 'O1' and 'O2' (their images are shown on the top right corner of Figure 1); their readout and erasing performances were detected and observed by two CCD monitors.

3. Results and discussion

3.1 Structure of multiple gratings

The intensities of the recording beams were adjusted to 1.05 mW/cm^2 by the attenuators, and the exposure time of 600 s was controlled by a valve. Two evident diffraction beam spots were detected during the exposure processing, indicating the formation of the multiple transmission grating. The morphology of the multiple-grating was observed by AFM (see Figure 2). As shown in the top view picture (Figure 2(a)), some regularly arranged stripe grooves are clearly discernable, indicating a satisfactory phase separation in PIPS. The periods of the ratings were tested according to side view analysis (Figure 2(b)); the larger one was about 4.3 μm, formed by the interference of L1 and L2, and the smaller was 1.0 μm, corresponding to the interference of the other beams, K1 and K2 with the polarised plane perpendicular to L1 and L2. By using Bragg's law, the periods of gratings, Λ, can be calculated theoretically, as expressed in the equation

$$\Lambda = \frac{\lambda_r}{2n_{\text{ave}} \sin \frac{\theta}{2}}, \tag{1}$$

in which, λ_r is the wavelength of holographic exposed source, 532 nm. The refractive index of grating medium, n_{ave}, measured by Abbe refractometer was 1.537. The cross-angle inside the medium, θ, is given in Section 2.2. Substituting these parameters into Equation (1), the grating pitches are obtained as 0.997 μm and 4.221 μm, when θ is 20° and 4.7°,

respectively. However, comparing with the periods measured through AFM a small difference is found, which is about 2.4% for $\theta = 20°$ and 2.0% for $\theta = 4.7°$. We believe that this comes from the volume shrinkage of the polymerisation during PIPS. A similar phenomenon has also been noted by Qi *et al.*, who reported that the shrinkage ratio is 2–4% [21], which is accordance with our results. Figure 2 also shows that except for the two gratings designed in the experiment, there is no other grating structure observed, which proves the rationality of our holography setup.

In addition, it is worth noting that the depth of grooves is only about 52 nm, as depicted in Figure 2(b), whereas the thickness of the medium is about 12 μm, which is 240 times the groove depth; this indicates that the grating shown in Figure 2 may be a surface relief structure. However, Figure 1 confirms that our experimental setup is a typical volume holographic exposure system. Thus, it was supposed that there may be some other volume gratings underneath the surface relief one. To clarify this, SEM was used to study the cross-section of the same sample. It is evident in Figure 3 that periodic LC-rich and polymer-rich zones are formed and run through the whole thickness of the sample film; the period is about 1 μm, which
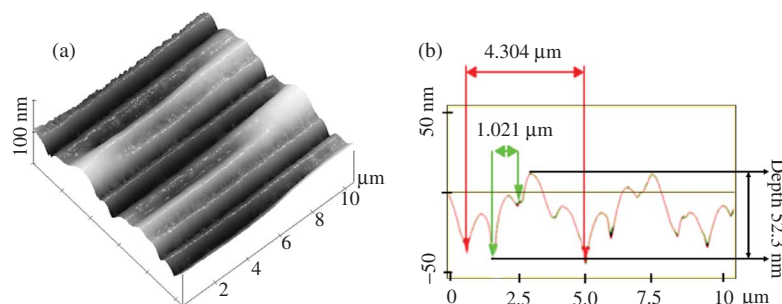

Figure 3.   Cross-section photograph of SEM.

Figure 2.   AFM photograph of multiple gratings. Top view (a) and side view (b).

is in accordance with the tested result of AFM, but it is hard to distinguish the multiple structure in this photograph. The thickness of the film was evaluated as about 12 μm, according to the scale at the lower right corner in Figure 3, which agrees with our cell gap. Thus the multiple gratings contain not only the volume holographic structure, but the surface relief. Such complicated structures also exist in other kinds of holographic grating based on conventional emulsions [22], but it has not previously been studied and reported in HPDLC. We believe that the formation of surface relief is related to the volume shrinkage of the grating; the larger the volume shrinkage is, the more evident surface relief appears.

3.2   Optical performance

The angular-dependent diffraction efficiencies of the multiple gratings were tested by a precisely controlled turntable. The diffraction spots and their intensities were detected and tested by the monitor-linked detector. As shown in Figure 4, two evident peaks appear as the incidence angle varies from $-8°$ to $24°$. The peak centre corresponds to the diffraction efficiency of Bragg incidence condition, and the Bragg angles of two gratings are $12°$ for grating G1 ($\Lambda = 1$ μm) and $2.9°$ for grating G2 ($\Lambda = 4.3$ μm). Theoretically, the Bragg angle satisfies

$$\theta_B = \sin^{-1}\left(\frac{\lambda_t}{2n_{ave}\Lambda}\right), \tag{2}$$

in which λ_t is represented as the tested wavelength, 633 nm in our experiments. Parameterisations of others are the same as the aforementioned. Thus, the calculated Bragg angles of grating G1 and G2 are $11.9°$
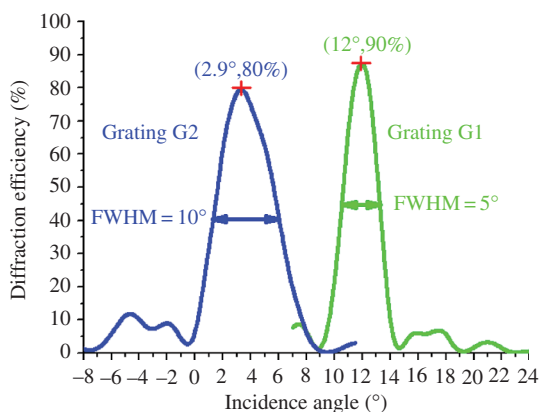
and $2.8°$, respectively, showing good agreement with the experimental data.

Figure 4 also shows the diffraction efficiency and full width at half maximum (FWHM) of two gratings. The grating with the larger period, G2, has lower diffraction efficiency and wider FWHM. This does not reflect poor optical performance of the grating; it may be related to the figure-of-merit (Q) [10], which is proportional to the thickness of the film (d) and inversely proportional to the square of period (Λ), and defined as

$$Q = 2\pi \frac{\lambda_t d}{n_{ave}\Lambda^2}. \tag{3}$$

Therefore, when the film thickness is constant, the grating with the larger period has a smaller figure-of-merit value, and the smaller the Q value is, the lower the diffraction efficiency and the wider the FWHM. According to this, the Q values of gratings G1 and G2 are calculated as 31.0 and 1.7, respectively, so the diffraction efficiency of G1 is 90%, which is 10% larger than G2, and the FWHM is $5°$, which is half of G2.

3.3   Electrical performance

The electrical tunability of two gratings was tested by applying a sine wave signal with 50 Hz frequency to the ITO cell. In this case, LC molecules align with the direction of the electrical field, and the diffractive index modulation of the gratings disappeared gradually with increasing applied voltage. The drive electric fields, V_{90}, defined as the applied field which makes the normalised diffraction efficiency decrease to the value of 0.9, are evaluated and given in Figure 5. The larger period grating (G2) has a relatively lower V_{90} value than the smaller period one (G1) because of the larger volume of LC droplets in G2 [23]. The tendencies of the two electro-optical curves are the same, with only a small difference between the drive electric fields;

Figure 4.   Angular dependent diffraction efficiencies of multiple gratings.
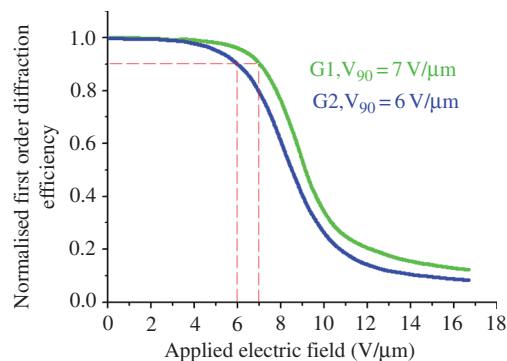

Figure 5.   Electro-optical behaviour of multiple gratings.

such results indicate a satisfied synchrony on electrically tunability. The tunable contrast ratios of the two gratings are over 5, which is necessary for applications such as displays and data storage.

3.4 Effects of structure on optical and electrical performance

It is mentioned above that the gratings contain the volume holographic structure and surface relief. The two structures can cause diffraction, but with different mechanisms; the former is a modulation of the refractive index between polymer and LCs, while the latter diffracts the beam through the geometrical modulations. So what about the effect of surface relief on the diffraction of the gratings? This was investigated as follows: the sample film was flushed with methanol several times to remove the LCs in the grooves of surface relief structure only, and then heated for 10 min at a temperature higher than the boiling point of methanol to evaporate the residual solutions. In order to eliminate the impact of the surface relief structure, the film was immersed in a refractive index-matching liquid (Cargille Series A, Cargille Laboratories, Inc.) with $n = 1.536$, which is approximately equal to the refractive index of the film, 1.537; the film was then sandwiched between two glass surfaces (the same as the glass of LC cell) and placed on the optical holder for testing.

The experimental results are given in Table 1. As shown, the diffraction efficiencies (DE) for gratings G1 and G2 decrease a little in the case where the surface relief is eliminated, and the rates of decrease are about 1.7% and 5% for G1 and G2, respectively. Our results are in accordance with those calculated through the Fourier modal method, in which the authors indicated that the diffraction of surface relief is less than 15% when the ratio of groove depth (d) and film thickness (D) satisfies $d/D < 1\%$, and the DE decreases exponentially with the ratio [24]. For our sample, the ratio is less than 0.4%, thus the effect of surface relief on DE is very weak. Therefore, it is believed that the volume structure (refractive index modulation) plays a major role in the DE of the gratings. The corresponding incidence angles at the maximum value of DE,

the Bragg angle θ_B, was tested; the results of the two gratings with and without surface relief are almost the same, because the Bragg angle is independent of surface relief. Some small decreases may be caused by the solution and refractive index-matching liquid, which change the structure of grating on the one hand and increase the refractive index modulation on the other hand. Sandwiching the same film between two glass surfaces with the ITO electrode on the inner surface, the drive electric fields of gratings were tested by applying the same wave signal mentioned in Section 3.3. The Kerr constant of the refractive index-matching liquid is very small, so the Kerr effect can be ignored in the test. Similarly, no evident changes occur, and some small decreases are related with the flush and immersion of the sample, which weaken the anchoring of polymer chain to the LC molecules.

3.5 Image storage

In order to study the application of HPDLC in multi-image storage, two transparent black and white plastic slices with different patterns ('O1' and 'O2') were placed at the labelled positions in Figure 1 and holographically recorded simultaneously. The readout and erasing performances of two images were tested by He–Ne laser. Figure 6 gives the pictures of two images without and with the applied electric field of 12 V/μm. As shown in Figures 6(a) and 6(b), the readout images are easily discerned and their edges are sufficiently clear. When a saturation field is applied on the film, two images can be electrically erased synchronously, as shown in Figures 6(c) and 6(d).

Figure 7 shows the intensity distributions of the images, analysed by two CCDs, and the local intensity is compared through the colour bar at the bottom. The distributions are similar to the corresponding images shown in Figure 6. The intensities of images

Table 1. Tested results of gratings with (sample A) and without (sample B) surface relief.

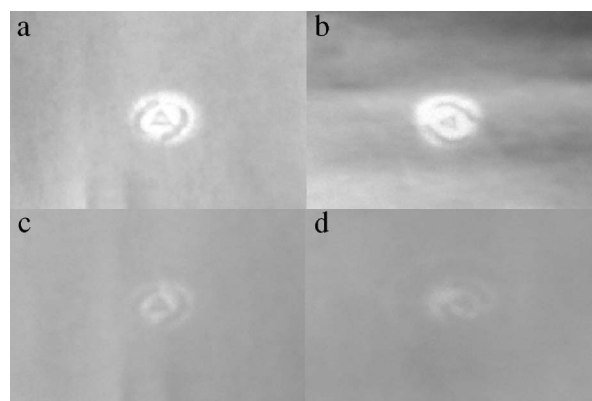| Sample		D.E.	θ_B	V_{90} (V/μm)
A	$G1_A$	90%	12°	7
	$G2_A$	80%	2.9°	6
B	$G1_B$	88.5%	11.8°	6.8
	$G2_B$	76%	2.8°	5.7

Figure 6. Images readout and electrically erasing. Pattern O1 (a) and (c), O2 (b) and (d).
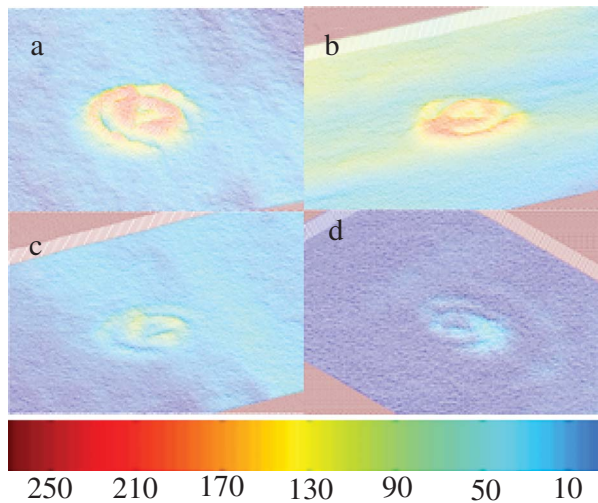
Figure 7. Intensity distribution of images readout and erasing. O1 (a) and (c), O2 (b) and (d). The colour bar of intensity is given at the bottom.

decrease as the electrical field is applied. The average intensities of image O1 and O2 are 245.7 a.u. (Figure 7(a)) and 224.8 a.u. (Figure 7(b)), respectively, and those of the erased are 29.3 a.u. (Figure 7(c)) and 21.4 a.u. (Figure 7(d)), respectively. The maximum tuneable contrast ratio for image O1 and O2 is evaluated as 8.4 and 10.5, respectively. Such contrast ratios agree very well with the results shown in Figure 5.

To investigate the potential application of such samples as displays, the transmission spectrum of the multi-image sample was tested with a visible spectrometer, as shown in Figure 8. Testing showed that the transmission of the sample was 77%, 85%, 91% and 98% at 450 nm, 500 nm, 550 nm and 625 nm, respectively. Thus we can estimate that the average transmission at red, green, blue bands is 81%, 88%, and 95%, respectively. These results indicate that the multiple recording sample is very suitable for low-end colour displays or for data storage. For high-end displays, some improvements should be made, for example,
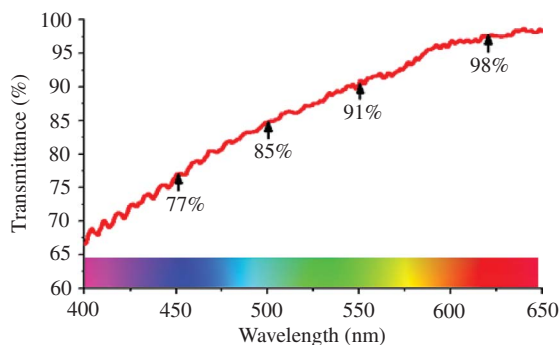
the tunable contrast ratio and the transmission at tri-colour should be increased, and the drive electric field should be lowered. Further studies are in progress.

4. Conclusions

Two transmission gratings with different periods were recorded simultaneously at the same position on HPDLC film by angular multiple holography setup. The optical and electrical performances of such multiple gratings were investigated and their structures were observed and tested with AFM and SEM technologies. Our results indicate that each grating in the multiple film contains not only a volume holographic structure, but also a surface relief. The effects of this surface relief on diffraction efficiency, Bragg angle and drive electric field of gratings were tested. Experimental data show that the diffractive performance of grating is mainly determined by the refractive index modulation in volume structure. The surface relief only diffracts 5% of the total diffraction energy. There are no evident effects of surface relief on the Bragg angle and drive electric field. In addition, about 2% of volume shrinkage is found because of polymerisation in PIPS. These results should be considered in the design of multiple HPDLC devices. Multiple image storage was also carried out by using the same exposure method. Image readout and erasing behaviours were detected and analysed by CCD, and their transmission at visible band was tested. These results show a prospective application of multiple HPDLCs as colour displays or in data storage.

Figure 8. Visible spectrum of multi-image HPDLC.

References

[1] Zhao, G.; Mouroulis, P. *J. Mod. Opt.* **1994**, *41*, 1929–1939.
[2] Piazzolia, S.; Jenkins, B.K. *J. Mod. Opt.* **1999**, *46*, 2079–2110.
[3] Brener, K.; Sauer, F. *Appl. Opt.* **1988**, *27*, 4251–4254.
[4] Natarajan, S.; Zhao, C.; Chen, R.T. *J. Lightwave Tech.* **1995**, *13*, 1031–1040.
[5] Piazzolia, S.; Jenkins, B.K.; Tanguay, A.R. *Opt. Lett.* **1992**, *17*, 676–678.

[6] Mok, F.H. *Opt. Lett.* **1993**, *18*, 915–917.

[7] Gambogi, W.J.; Weber, A.M.; Trout, T.J. *Proc. SPIE* **1993**, *2043*, 2–13.

[8] Colvin, V.L.; Larson, R.G.; Harris, A.L.; Schilling, M.L. *J. Appl. Phys.* **1997**, *81*, 5913–5923.

[9] Mucha, M. *Prog. Polym. Sci.* **2003**, *28*, 837–873.

[10] Bunning, T.J.; Natarajan, L.V.; Tondglia, V.P.; Sutherland, R.L. *Ann. Rev. Mater. Sci.* **2000**, *30*, 83–115.

[11] Sutherland, R.L.; Natarajan, L.V.; Tondiglia, V.P.; Bunning, T.J. *Chem. Mater.* **1993**, *5*, 1533–1538.

[12] Yamamoto, T.; Hasegawa, M.; Kanazawa, A.; Shiono, T.; Ikeda, T. *J. Mater. Chem.* **2000**, *10*, 337–342.

[13] Xia, T.; Guang, W.; Artashes, Y.; Tigran, G.; Yue, Z. *Adv. Mater.* **2005**, *17*, 370–374.

[14] Bang, C.U.; Shishido, A.; Ikeda, T.; Kurihara, H. *Mol. Cryst. Liq. Cryst.* **2006**, *458*, 149–159.

[15] Bowley, C.C.; Fontecchio, A.K.; Crawford, G.P.; Lin, J.J.; Li, L.; Faris, S. *Appl. Phys. Lett.* **2000**, *76*, 523–525.

[16] Date, M.; Takeuchi, Y.; Kato, K. *J. Phys. D: Appl. Phys.* **1999**, *32*, 3164–3168.

[17] Caputo, R.; Sio, L.D.; Veltri, A. *J. Disp. Tech.* **2006**, *2*, 38–51.

[18] Massenot, S.; Kaiser, J.L.; Perez, M.C.; Chevallier, R.; de Bougrenet de la Tocnaye, J.L. *Appl. Opt.* **2005**, *44*, 5273–5280.

[19] Crawford, G.P. *Opt. Photonics News* **2003**, *14*, 54–59.

[20] Liu, Y.J.; Sun, X.W. *Adv. OptoElectronics* **2008**, 684349. doi: 10.1155/2008/684349

[21] Qi, J.; DeSarkar, M.; Warren, G.T.; Crawford, G.P. *J. Appl. Phys.* **2002**, *91*, 4795–4800.

[22] Moharam, M.G.; Gaylord, T.K. *J. Opt. Soc. Am.* **1981**, *71*, 811–818.

[23] Wu, B.G.; Erdmann, J.H.; Doane, J.W. *Liq. Cryst.* **1989**, *5*, 1453–1465.

[24] Li, L.F. *J. Opt. Soc. Am. A* **1993**, *10*, 2581–2591.